Body-Deformation Steering Approach to Guide a Multi-mode Amphibious Robot on Land

Qinghai Yang, Junzhi Yu, Rui Ding, and Min Tan

Key Laboratory of Complex Systems and Intelligence Science,
Institute of Automation, Chinese Academy of Sciences, Beijing 100190, China
qinghai.yang@ia.ac.cn

Abstract. This paper addresses the locomotion control for a biomimetic amphibious robot capable of multi-mode motion both in water and on land. Currently, a wheel-like device named wheel-paddle is employed as the primary driving mode. Depending on the deflections of rear propelling units, a body-deformation based steering approach is proposed, and an optimal realization is explored through geometrical analysis. Furthermore, the kinematic models as well as corresponding simulation results are outlined and the error between two models is also summarized. The experimental results demonstrate the validity, stability and maneuverability of the formed steering, satisfying robot's operation requirements on land.

Keywords: Amphibious robot, locomotion control, body-deformation steering, kinematic models.

1 Introduction

Amphibian animals, as the most primitive terrestrial vertebrate, endure the long natural selection and are the transitional animals in vertebrate's evolution from aquatic vertebrate to terrestrial one, which acquires not only the inherited characteristics suitable for aquatic living, but also the new features adapted to living on land. Attractively, the amphibian has excellent adaptability to various environments, which offers good ideas in developing bio-inspired robots.

With the research domain and activity field extending gradually, all kinds of robots emerge, most of which are single functioned robots. In particular, the amphibious robots capable of operations both on ground and in water are relatively rare. The existing amphibious robots mainly adopt legged motion and snake-like motion as their driving method on land [1]. Some legged amphibious robots include the lobster robot of Northeastern University of US [2], and the ALUV by IS Robotics and Rockwell [3]. To expand the limited operation in the seabed and avoid the complicated control algorithm, some improved legged structures are adopted as major driving devices, such as the simplified wheel-leg propellers of Wheg IV in Case Western Reserve University and Naval Postgraduate School [4], the actuated fins of robotic turtle in Nekton Research [5], and the paddles and semicircular legs used by a series of legged amphibious robots developed by McGill University and its cooperative university [6]. Due to multiple locomotion modes and biological features surviving in various

C. Xiong et al. (Eds.): ICIRA 2008, Part I, LNAI 5314, pp. 1021–1030, 2008.

terrains, snake-like locomotion mode is also utilized as amphibious locomotor in robotics, for instance, ACM-R5 by Tokyo Institute of Technology and AmphiBot by Swiss Federal Institute of Technology [7], [8]. The reliable watertight structures and multifunctional driving mechanisms, at present, are the primary difficulties faced by amphibious robots.

Based on research results on mechatronic design and motion control of biomimetic robotic fish/dolphin [9], [10], this paper presents our achievements to create an amphibious robot, "AmphiRobot", which is capable of multi-mode motion. By importing module-based design methodology, the robot is constructed out of a head, multiple identical propelling-units, and a flapping foil, which allows flexible propulsion and reliable maintenance. Compared with the existing amphibious robots, the multi-purpose, amphibious propulsive mechanism that combines carangiform or dolphin-like swimming and wheel-like motion makes efficient movements both under water and on ground possible. The amphibious robot can be employed in many applications such as ecological monitoring, safety check, aquiculture, search and rescue, military purpose, etc., in surf zones and harbors.

The rest of the paper is organized as follows. Section 2 describes the overall structure and the mechanical configuration of the robotic prototype. The steering analysis based on the geometry and comparison of three steering methods is addressed in Section 3. In Section 4, the kinematics model and simulation, along with corresponding experimental results, are presented. Section 5 concludes the paper with the summary about the current robot and an outline of future work.

2 Mechanical Design

Fish swimming in nature by the coordinate motion of its body, fins, and tail, achieves tremendous propulsive efficiency and excellent maneuverability that have great advantage over conventional marine vehicles. Dolphin also exhibits an astonishing level of swimming capabilities by vertical fluke oscillations which are different with those of fish tail in the horizontal plane and endow dolphin with better maneuverability than lateral oscillations of fish in vertical plane.

The AmphiRobot takes inspiration of undulatory/oscillatory body motions of fish and possesses several modular body links and a large aspect ration lunate tail. In water, AmphiRobot uses a flexible posterior body and an oscillating foil as a propulsor and swims just like a fish. In the meantime, an agile swiveling body device makes it possible to convert the motion of modular links and tail in horizontal plane into the movement in vertical plane, and realize the dolphin-like swimming.

2.1 General Structure

AmphiRobot, as shown in Fig. 1, is composed of a head and a series of identical joints, called modular propelling-units. The shell frames of whole robot are manufactured using aluminum alloy for its high strength-to-weight ratio as well as its high thermal conductivity. The side covers of the head and units are made of polymethyl methacrylate, so the transparence will allow convenient leakage detection as well as the inspection of components' working states.

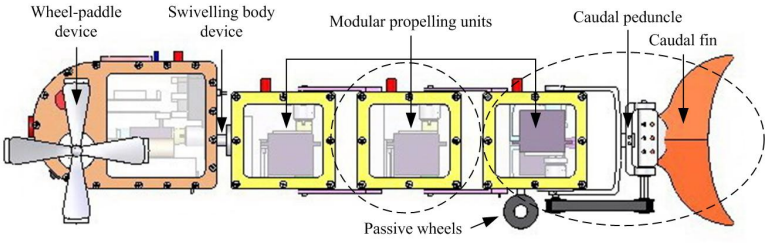

Fig. 1. Front view of an amphibious robot capable of multi-mode motion

There is a special part in the head, called swivelling body device, which is driven by a servomotor and can revolve all of the posterior propelling-units in ±90°. When the swivelling device moves to the ultimate position of +90°, the AmphiRobot implements the switch from the fish-swimming mode to dolphin-swimming mode.

2.2 Driving Device on Land

In water, a pair of flippers shown in Fig. 2 (a) is fixed to the actuating shafts, acting as pectoral fins and assisting the propelling-units to implement moving forward, turning, and pitching by jigging motion. When the robot comes out from water, the flippers turn into limbs functionally and their continuous rotation makes AmphiRobot "crawl" forward. Apparently, the "crawling" speed on the ground is very slow and insufficient for the operation on land, and a new driving mode is necessary to be developed.

There are many locomotion devices available on land, such as wheel, leg, track, etc. Among them, wheeled mobile mechanism has a long history and is very popular in all kinds of mobile robots because of its mature mechanical design and simple control algorithm. Considering the whole structure of AmphiRobot, actuating method and the implementation difficulty, a pair of wheel-like devices named wheel-paddles with four spokes and four feet at the end of spokes, as depicted in Fig. 2 (b), is employed and assembled in each side of the robot's head. The similarity with wheel on structure turns crawling motion into rolling motion and makes up the deficiency of the flipper. According to the actual construction of the robot and application field, a pair of passive rubber tires is utilized and mounted in the bottom of the last propelling unit, which reduces the friction force greatly and combines the high locomotion speed and excellent stability together.

(a) (b)

Fig. 2. The alternative flipper and wheel-paddle. (a) The flipper driving the robot "crawl" on land. (b) The wheel-paddle with a heterotypic structure, acting as the primary driving mode on land.

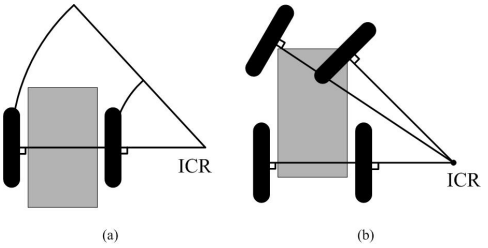

Fig. 3. Two locomotion modes for mobile robots on land. (a) The differential drive, where the speed difference between left and right wheels forms an ICR. (b) The ackerman steering, where the inside front wheel is rotated slightly sharper than the outside wheel, and the two mutually independent wheels, along with the rear passive wheels forms a fixed ICR.

The choice of wheel-paddles rather than wheels is that the wheel-paddle can climb on higher obstacle than wheels. The obstacle performance is relative to the radius of driving wheels, bigger wheels allow overcoming higher obstacles, but they require higher torque or reductions in the gear box. With consideration to the obstacle performance and the output torque of motor combination, the radius of the wheel-paddles is determined to 65 mm. Notice that the compatibility of flippers and wheel-paddles meets the diverse demands, and that suitable component will be selected in terms of specific working conditions.

3 Steering Analysis Based on Geometry

The mobile robot locomotion on land involves differential drive, steered wheel drive, synchronous drive, omni-directional drive and ackerman steering. AmphiRobot has two driving wheel-paddles and it seems that the differential drive in Fig. 3 (a) is a reasonable locomotion form for the robot. But, the quite long body of robot and the lateral friction of rear passive wheels have somewhat negative influence to steering. The poor actual steering performance verifies the incongruity of differential steering.

As shown in Fig. 3 (b), the structure of AmphiRobot is similar to that of car drive. The perpendiculars of two mutually independent wheels and the fixed wheels of a car form an instantaneous center of rotation (ICR) and the orientation of the car will be changed. When the robot body remains straight, the fore driving wheel-paddles and rear passive wheels are parallel, no ICR is formed, and the robot moves forward. Benefiting greatly from the carangiform swimming mode in water, the robot's body shape can be changed when the modular propelling units departure from their central positions, and then the perpendiculars of wheel-paddles and passive wheels intersect and an ICR is formed which makes the robot maneuver on land. We define the applied turning method on land as body-deformation steering.

The rotations of the second or third unit independently and the coordinated oscillations of the two units will make the body shape change and satisfy the requirements of forming an ICR. So there exist three ways available to steer the robot agilely on land. These three methods form different ICRs which correspond to different turning radii, and the following part will analyze these methods and try to seek an optimal one.

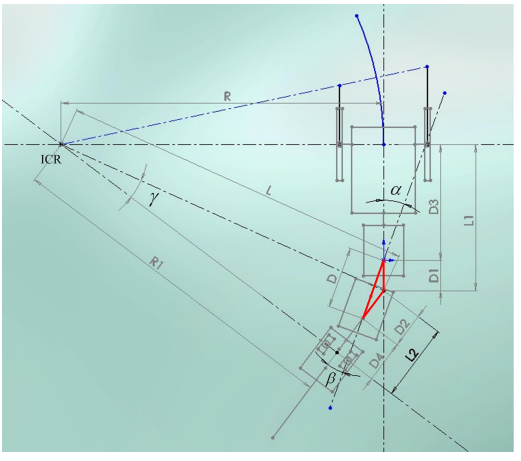

Fig. 4. The change of body shape by the coordinated deflections of the second and third propelling units. The perpendiculars of wheel-paddles and passive wheels form an ICR, and the robot will turn left.

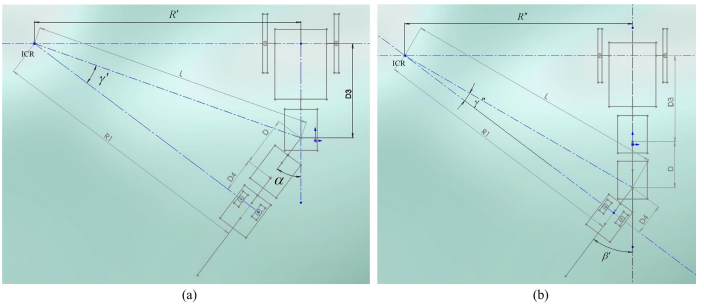

Fig. 5. The deflection of the second or third propelling unit separately changes the body shape and forms new ICRs. (a) and (b) correspond to the separate rotating of the second and third unit.

3.1 Coordinated Deflection Via the Last Two Propelling Units

As shown in the Fig. 4, both the second unit and the third one departure from their middle positions with offset of α and β, respectively. The body shape turns from a straight line into an approximate arc shape and an ICR is formed.

Once the deflection angles of propelling units are given, $D1$ and $D2$ can be calculated based on the relation of side length and interior angle of triangle as

$$\frac{D1}{\sin\beta} = \frac{D}{\sin(\pi-\alpha-\beta)} \quad \frac{D2}{\sin\alpha} = \frac{D}{\sin(\pi-\alpha-\beta)}. \tag{1}$$

where D is a constant.

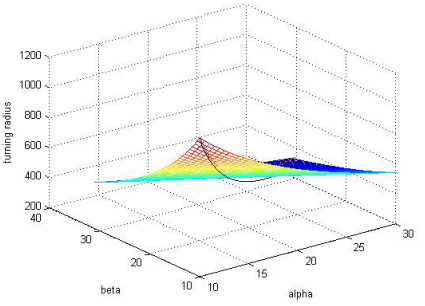

Fig. 6. Comparative result for three methods to form ICR. The hood face is the turning radius corresponding to coordinated deflection of the second and third units. The red and black curves denote the turning radii corresponding to the independent deflection of the second and third units. The unit of deflection angle and turning radius are degree and millimeter respectively.

The two right triangles share the same hypotenuse, so we can get

$$\begin{cases} \sin(\alpha+\beta-\gamma)=\dfrac{L1}{L} \\ \sin\gamma=\dfrac{L2}{L} \end{cases} \Rightarrow \frac{L1}{\sin(\alpha+\beta-\gamma)}=\frac{L2}{\sin\gamma}. \tag{2}$$

where $L1 = D1 + D3$, $L2 = D2 + D4$, particularly $D3$ and $D4$ are known variables.

With (1)~(2), γ can be solved, and then the turning radius corresponding to the specific deflection can be given through $R = L1*\cot(\alpha+\beta-\gamma)$ as

$$R=\frac{D\left(\sin\alpha+\sin\beta*\cos\left(\alpha+\beta\right)\right)+D3*\sin\left(\alpha+\beta\right)*\cos\left(\alpha+\beta\right)+D4*\sin\left(\alpha+\beta\right)}{\sin^2\left(\alpha+\beta\right)}. \tag{3}$$

3.2 Deflection of the Second or Third Propelling Unit Separately

The separate rotating of the second or third unit can also form ICR, as show in Fig. 5. According to the above calculation method, we can get the R' and R''

$$R'=\frac{D3*\cos\alpha+D+D4}{\sin\alpha} \quad R''=\frac{\left(D+D3\right)\cos\beta+D4}{\sin\beta}. \tag{4}$$

3.3 Comparison of Three Methods

In order to get the optimal turning method, we compare the radii of three turning ways on the same deflection angels, that is

$$\alpha+\beta=\alpha'=\beta'. \tag{5}$$

The comparative result is show in Fig. 6, and can be expressed as

$$R''<R<R'. \tag{6}$$

With the same deflections, the case employing the third propelling unit to rotate around its spin axis generates the minimal radius, in which the robot is more maneuverable on land.

3.4 Differekntial Velocity

Assume that the revolutions, angular velocities and linear velocities of the left and right wheel paddles are n_L, n_R, ω_L, ω_R, and V_L, V_R, respectively, the angular velocity of the robot is ω. As can be observed in Fig. 4, the left and right wheel-paddles have the same angular velocity and different linear velocity, that is

$$\begin{cases} V_R = r\omega_R = r\dfrac{2\pi n_R}{60} = \omega * \left(R'' + \dfrac{d}{2} \right) \\ V_L = r\omega_L = r\dfrac{2\pi n_L}{60} = \omega * \left(R'' - \dfrac{d}{2} \right) \end{cases}. \tag{7}$$

where r is the radius of wheel-paddle and d is the distance between the two wheel-paddles. Then (7) yields

$$\frac{n_R}{n_L} = \frac{R'' + \dfrac{d}{2}}{R'' - \dfrac{d}{2}}. \tag{8}$$

And this is the relationship of revolutions of the two wheel-paddles when steering.

4 Kinematic Models and Experimental Result

4.1 Kinematic Models

Base on the optimal body-deformation steering by the deflection of the third propelling unit, the two robot frames are established in the midpoints of the rear wheels and

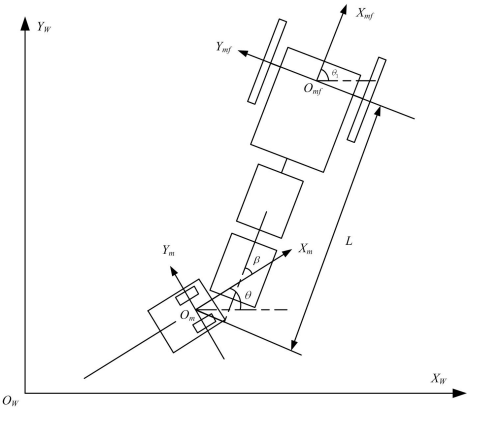

Fig. 7. The kinematic model based on the body-deformation steering

forward wheel-paddles, taking the heading of the third propelling unit and head module as the orientations of X axis, and the orientations from right wheel to left wheel as that of Y axis, as shown in Fig. 7.

Then we can establish the equation below

$$\begin{cases} \dot{x} = v\cos(\theta + \beta) \\ \dot{y} = v\sin(\theta + \beta) \end{cases}. \tag{9}$$

where v is the motion speed of midpoint of driving wheel-paddles; θ is the direction angle, namely, the angle between X_m and X_W; β is the steering angle of guide wheels; $\dot{x}$ and $\dot{y}$ are the translational velocities of O_{mf}.

Though the rotating of the third unit causes deviation of passive wheels from the longitudinal central line, the offset is very little compared with the distance between fore and rear wheels, therefore we can get another equation approximately as

$$\dot{\theta} = (v / L)\tan\beta . \tag{10}$$

where L is the distance between the two midpoints, and $\dot{\theta}$ is the rotary velocity.

The equations (9) and (10) compose one of the kinematic models of the robot.

Due to the special steering method, the rear wheels have different radius with that of fore wheel-paddles, another kinematic model can be expressed below

$$\begin{cases} \dot{x}' = v\cos(\theta + \beta) + v\tan\beta\sin(\theta + \beta) \\ \dot{y}' = v\sin(\theta + \beta) + v\tan\beta\cos(\theta + \beta) \\ \dot{\theta} = (v / L)\tan\beta \end{cases}. \tag{11}$$

where $\dot{x}'$ and $\dot{y}'$ are the translational velocities of O_m in the world frame.

Based on the kinematic equations (9), (10) and (11), we can have the locomotion routes which are shown in Fig. 8. The circle in blue asterisk is the track of fore wheel-paddles, and the red one is that of rear passive wheels. The error between the two tracks presented in the figure is caused by the approximation of (10), which is the departure of midpoint of rear wheels from the longitudinal centerline.

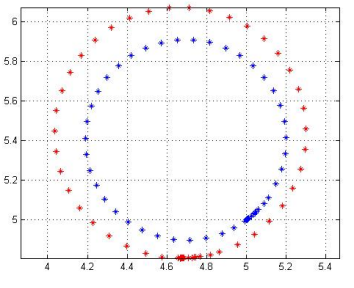

Fig. 8. The simulation result of two kinematic models

Fig. 9. The circular motion achieved by body-deformation steering. The anticlockwise snapshots show the different moving positions in a circle successively. The blue and red lines in two captures denote the same locations in the actual ground.

4.2 Experimental Results

To verify the body-deformation steering approach and the analysis about the turning radius, we performed some experiments on the ceramic tile-paved floor in our lab. During experiments, the head and the first two propelling units keep in a straight line, the third unit is rotated by a specific angle of 37° which remains the same all the while, with the velocities of the left and right wheel-paddles according with the relationship in (8), and a circular motion is gained, as shown in Fig. 9. The actual steering radius is about 550 mm, and the calculated radius from (4) is 552 mm. The negligible error between the theoretical and experimental performance demonstrates the validity of the utilized body-deformation steering approach.

5 Conclusions and Future Work

In this paper, a geometry based steering method named body-deformation steering, aiming at ground movements, has been designed for a multi-mode amphibious robot equipped with wheel-paddles and passive wheels. Two kinematic models compatible with this special robotic construction and their simulation routes have been formed, and the possible reasons for generated error have been summarized. The comparative results have partly validated the feasibility and maneuverability of the proposed steering approach.

Further research will concentrate on investigating obstacle avoidance, path planning and intelligent control on land. More effects, of course, will be paid to achieve autonomous locomotion control in water.

Acknowledgement

This work was supported in part by the National Natural Science Foundation of China (Grant Nos 60505015 and 60775053), in part by the Beijing Natural Science Foundation

under Grant 4082031, in part by the National 863 Program under Grant 2007AA04Z202, and in part by the CASIA Innovation Fund for Young Scientists.

References

1. Yang, Q., Yu, J., Tan, M., Wang, S.: Amphibious biomimetic robots: a view. Robot 29, 601–608 (2007)
2. Ayers, J.: Underwater walking. Arthropod structure & development 33, 347–360 (2004)
3. Greiner, H., Shectman, A., Won, C., Elsley, R., Beith, P.: Autonomous legged underwater vehicles for near land warfare. In: IEEE Symposium on Autonomous Underwater Vehicle Technology, pp. 41–48. IEEE Press, Piscataway (1996)
4. Boxerbaum, A.S., Werk, P., Quinn, R.D., Vaidyanathan, R.V.: Design of an autonomous amphibious robot for surf zone operation: Part I mechanical design for multi-mode mobility. In: 2005 IEEE/ASME International Conference on Advanced Intelligent Mechatronics, Monterey, pp. 1460–1464 (2005)
5. Kemp, M., Hobson, B., Long, J.H.: Madeleine: an agile AUV propelled by flexible fins. In: 14th International Symposium on Unmanned Untethered Submersible Technology, New Hampshire, pp. 1–6 (2005)
6. Prahacs, C., Saunders, A., Smith, M.K., McMordie, D., Buehler, M.: Towards legged amphibious mobile robotics. In: The Inaugural Canadian Design Engineering Network (CDEN) Design Conference (2004)
7. Yamada, H., Chigisaki, S., Mori, M., Takita, K., Ogami, K., Hirose, S.: Development of amphibious snake-like robot ACM-R5. In: 36th Int. Symposium on Robotics, Tokyo, pp. 433–440 (2005)
8. Crespi, A., Badertscher, A., Guignard, A., Ijspeert, A.J.: AmphiBot I: an amphibious snake-like robot. Robotics and Autonomous Systems 50, 163–175 (2005)
9. Yu, J., Hu, Y., Fan, R., Wang, L., Huo, J.: Mechanical design and motion control of a biomimetic robotic dolphin. Advanced Robotics 21, 499–513 (2007)
10. Yu, J., Tan, M., Wang, S., Chen, E.: Development of a biomimetic robotic fish and its control algorithm. IEEE Trans. on System, Man, and Cybernetics-Part B: Cybernetics 34, 1798–1810 (2004)